35th International Symposium on Lattice Field Theory, 18-24 June 2017, Granada, Spain

Singlet vs Nonsinglet Perturbative Renormalization factors of Fermion Bilinears

Gregoris Spanoudes and Haris Panagopoulos

Department of Physics, University of Cyprus, POB 20537, 1678, Nicosia, Cyprus

INTRODUCTION

In this poster we present the perturbative computation of **the difference between the renormalization factors of flavor singlet ($\sum_f \bar{\psi}_f \Gamma \psi_f$, f: flavor index) and nonsinglet ($\bar{\psi}_{f_1}\Gamma\psi_{f_2}$, $f_1 \neq f_2$) bilinear quark operators** (where $\Gamma = 1\!\!1, \gamma_5, \gamma_\mu, \gamma_5\gamma_\mu, \gamma_5\sigma_{\mu\nu}$) on the lattice. The computation is performed to **two loops** and to lowest order in the lattice spacing, using **Symanzik improved gluons** and **staggered fermions with twice stout-smeared links**. The stout smearing procedure is also applied to the definition of bilinear operators. A significant part of this work is the development of a method for treating some new peculiar divergent integrals stemming from the staggered formalism. Our results can be combined with precise simulation results for the renormalization factors of the nonsinglet operators, in order to obtain an estimate of the renormalization factors for the singlet operators. The corresponding calculation with SLiNC fermions had been previously performed by our group [1]. The results have been published in Physical Review D [2].

Flavor singlet operators are relevant for a number of hadronic properties including, e.g., topological features or the spin structure of hadrons. Matrix elements of such operators are notoriously difficult to study via numerical simulations, due to the presence of (fermion line) disconnected diagrams, which in principle require evaluation of the full fermion propagator. Then **it is quite a challenge to obtain accurate results for the renormalization of the singlet operators** directly. In recent years there has been some progress in the numerical study of flavor singlet operators; furthermore, for some of them, a **nonperturbative estimate** of their renormalization has been obtained using the **Feynman-Hellmann relation** [3]. Perturbation theory can give an important cross check for these estimates, and provide a prototype for other operators which are more difficult to renormalize nonperturbatively. Given that the renormalization factors of the nonsinglet operators can be calculated nonperturbatively with quite good precision, we can give an **estimate of the renormalization factors for the singlet operators through the perturbative evaluation of the difference between singlet and nonsinglet cases**.

Staggered fermions entail additional complications as compared to Wilson fermions. In particular, the fact that fermion degrees of freedom are distributed over neighbouring lattice points requires the **introduction of link variables in the definition of gauge invariant fermion bilinears**, with a corresponding increase in the number of Feynman diagrams. In addition, the appearance of **16 (rather than 1) poles in the fermion propagator** leads to a rather intricate structure of divergent contributions in two-loop diagrams.

A novel aspect of the calculations is that the gluon links, which appear both in the staggered fermion action and in the definition of the staggered bilinear operators, are improved by applying a stout smearing procedure up to two times, iteratively. Compared to most other improved formulations of staggered fermions, the **stout smearing action** leads to **smaller taste violating effects** [4–6]. Application of stout improvement on staggered fermions thus far has been explored, by our group, only to one-loop computations [7]; a two-loop computation had never been investigated before.

LATTICE ACTIONS

In our calculation we made use of the **staggered formulation of the fermion action** on the lattice, applying a twice stout smearing procedure on the gluon links. In standard notation, it reads:

$$S_{\rm SF} = a^4 \sum_{x,\mu} \frac{1}{2a}\bar{\chi}(x)\,\eta_\mu(x)\left[\tilde{\tilde{U}}_\mu(x)\,\chi(x+a\hat{\mu}) - \tilde{\tilde{U}}^\dagger_\mu(x-a\hat{\mu})\,\chi(x-a\hat{\mu})\right] + a^4\sum_x m\,\bar{\chi}(x)\,\chi(x) \tag{1}$$

where $\chi(x)$ is a one-component fermion field, and $\eta_\mu(x) = (-1)^{\sum_{\nu<\mu} n_\nu}$ $[x = (a\,n_1, a\,n_2, a\,n_3, a\,n_4),\quad n_i \in \mathbb{Z}]$. The relation between the staggered field $\chi(x)$ and the standard fermion field $\psi(x)$, is given by:

$$\psi(x) = \gamma_x\,\chi(x), \quad \bar{\psi}(x) = \bar{\chi}(x)\,\gamma_x^\dagger \tag{2}$$

where $\gamma_x = \gamma_1^{n_1}\gamma_2^{n_2}\gamma_3^{n_3}\gamma_4^{n_4}$. Since a single fermion field component $\chi(x)$ corresponds to each lattice site, the staggered action contains 4 rather than 16 fermion doublers, which are called "tastes". Then, a physical fermion field $\psi(x)$ with taste components (totally 16 components) lives in a 4-dimensional unit hypercube of the lattice. The gluon links $\tilde{\tilde{U}}_\mu(x)$, appearing above, are **"doubly" stout links**, defined as:

$$\tilde{\tilde{U}}_\mu(x) = e^{i\,\tilde{Q}_\mu(x)}\,\tilde{U}_\mu(x) \tag{3}$$

where $\tilde{U}_\mu(x)$ is the "singly" stout link [8]:

$$\tilde{U}_\mu(x) = e^{i\,Q_\mu(x)}\,U_\mu(x)\,, \tag{4}$$

$$Q_\mu(x) = \frac{\omega}{2\,i}\left[V_\mu(x)U_\mu^\dagger(x) - U_\mu(x)V_\mu^\dagger(x) - \frac{1}{N_c}{\rm Tr}\left(V_\mu(x)U_\mu^\dagger(x) - U_\mu(x)V_\mu^\dagger(x)\right)\right], \tag{5}$$

$$V_\mu(x) = \sum_{\rho=\pm1}^{\pm4} U_\rho(x)U_\mu(x+a\hat{\rho})U_\rho^\dagger(x+a\hat{\mu}) \tag{6}$$

$V_\mu(x)$ represents the sum over all staples associated with the link $U_\mu(x)$, ω is a tunable parameter, called stout smearing parameter and N_c is the number of colors. Correspondingly, $\tilde{Q}_\mu(x)$ is defined as in Eq.(5), but using $\tilde{U}_\mu$ as links (also in the construction of V_μ). To obtain results that are as general as possible, we use different stout parameters, ω, in the first (ω_1) and the second (ω_2) smearing iteration.

For gluons, we employ a **Symanzik improved action**, of the form [9]:

$$S_G = \frac{2}{g_0^2}\Big[\ c_0\sum_{\rm plaq.}{\rm Re\,Tr}\{1-U_{\rm plaq.}\} + c_1\sum_{\rm rect.}{\rm Re\,Tr}\{1-U_{\rm rect.}\} + c_2\sum_{\rm chair}{\rm Re\,Tr}\{1-U_{\rm chair}\} + c_3\sum_{\rm paral.}{\rm Re\,Tr}\{1-U_{\rm paral.}\}\Big] \tag{7}$$

where $U_{\rm plaq.}$ is the 4-link Wilson loop and $U_{\rm rect.}$, $U_{\rm chair}$, $U_{\rm paral.}$ are the three possible independent 6-link Wilson loops (see Fig. 1).

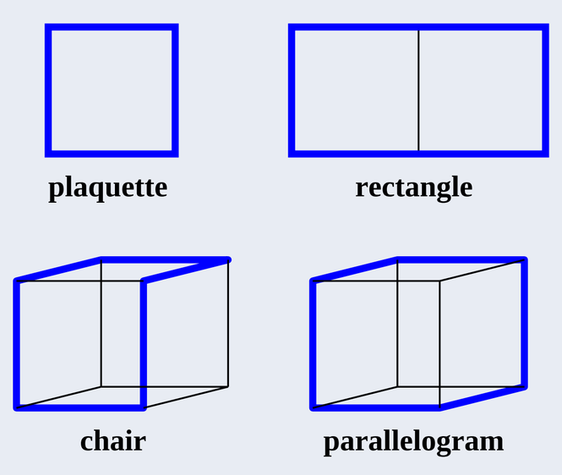

Figure 1: The 4 Wilson loops of the gluon action.

The Symanzik coefficients c_i satisfy the following normalization condition:

$$c_0 + 8c_1 + 16c_2 + 8c_3 = 1 \tag{8}$$

We have selected a number of commonly used sets of values for c_i, some of which are shown in Table 1.

Gluon action	c_0	c_1	c_2	c_3
Wilson	1	0	0	0
TL Symanzik	5/3	-1/12	0	0
Iwasaki	3.648	-0.331	0	0

Table 1: Selected sets of values for Symanzik coefficients.

DEFINITION OF STAGGERED FERMION BILINEAR OPERATORS

In the staggered formalism, each physical fermion field component $\psi_{\alpha,t}$ (where α is a Dirac index and t is a taste index) is defined as a linear combination of the single-component fermion fields χ that live on the corners of 4-dimensional elementary hypercubes of the lattice. In standard notation:

$$\psi_{\alpha,t}(y) = \frac{1}{2}\sum_C (\gamma_C)_{\alpha,t}\,\chi_C(y)\,, \quad \chi_C(y) = \frac{1}{2}\sum_{\alpha,t}(\xi_C)_{\alpha,t}\,\psi_{\alpha,t}(y) \tag{9}$$

where $\chi_C(y) \equiv \chi(y+aC)/4$, y denotes the position of a hypercube inside the lattice ($y_\mu \in 2\mathbb{Z}$), C denotes the position of a fermion field component within a specific hypercube ($C_\mu \in \{0,1\}$), $\gamma_C = \gamma_1^{C_1}\gamma_2^{C_2}\gamma_3^{C_3}\gamma_4^{C_4}$ and $\xi_C = \xi_1^{C_1}\xi_2^{C_2}\xi_3^{C_3}\xi_4^{C_4}$, $\xi_\mu = \gamma_\mu^*$.

Using Eq.(9), one can define the fermion bilinear operators $\mathcal{O}_{\Gamma,\Xi} = \bar{\psi}(y)\ (\Gamma\otimes\Xi)\ \psi(y)$ (where Γ and Ξ are arbitrary 4×4 matrices acting on the Dirac and taste indices of $\psi_{\alpha,t}(y)$, respectively) in terms of the staggered fermion fields $\chi_C(y)$ [10]:

$$\mathcal{O}_{\Gamma,\Xi} = \sum_{C,D}\bar{\chi}_C(y)\,\frac{1}{4}\,{\rm Tr}\left[\gamma_C^\dagger\,\Gamma\,\gamma_D\,\Xi\right]\,U_{C,D}\,\chi_D(y)\,, \tag{10}$$

where one inserts the quantity $\boldsymbol{U_{C,D}}$, which is the average of products of gauge link variables along all possible shortest paths connecting the sites $y+C$ and $y+D$, in order to restore gauge invariance.

Using the relations $\gamma_\mu\gamma_C = \eta_\mu(C)\gamma_{C+\hat{\mu}}$ and tr $(\gamma_C^\dagger\gamma_D) = 4\delta_{C,D}$, the **taste-singlet staggered fermion bilinear operators** take the following form:

$$\mathcal{O}_S(y) = \sum_D \bar{\chi}_D(y)\,\chi_D(y) \tag{11}$$

$$\mathcal{O}_V(y) = \sum_D \bar{\chi}_{D+_2\hat{\mu}}(y)\,U_{D+_2\hat{\mu},D}\,\chi_D(y)\,\eta_\mu(D) \tag{12}$$

$$\mathcal{O}_T(y) = \frac{1}{i}\sum_D \bar{\chi}_{D+_2\hat{\mu}+_2\hat{\nu}}(y)\,U_{D+_2\hat{\mu}+_2\hat{\nu},D}\,\chi_D(y)\,\eta_\nu(D)\,\eta_\mu(D+_2\hat{\nu})\,,\ \mu\neq\nu \tag{13}$$

$$\mathcal{O}_A(y) = \sum_D \bar{\chi}_{D+_2\hat{\mu}+_2(1,1,1,1)}(y)\,U_{D+_2\hat{\mu}+_2(1,1,1,1),D}\,\chi_D(y)\,\eta_\mu(D)\,\cdot\ \eta_1(D+_2\hat{\mu})\,\eta_2(D+_2\hat{\mu})\,\eta_3(D+_2\hat{\mu})\,\eta_4(D+_2\hat{\mu}) \tag{14}$$

$$\mathcal{O}_P(y) = \sum_D \bar{\chi}_{D+_2(1,1,1,1)}(y)\,U_{D+_2(1,1,1,1),D}\,\chi_D(y)\,\eta_1(D)\,\eta_2(D)\,\eta_3(D)\,\eta_4(D) \tag{15}$$

where $a +_2 b \equiv (a+b)$ mod 2 and $\boldsymbol{S}$**(Scalar)**, $\boldsymbol{P}$**(Pseudoscalar)**, $\boldsymbol{V}$**(Vector)**, $\boldsymbol{A}$**(Axial Vector)**, $\boldsymbol{T}$**(Tensor)** correspond to: $\boldsymbol{\Gamma = 1\!\!1, \gamma_5, \gamma_\mu, \gamma_5\gamma_\mu, \gamma_5\,\sigma_{\mu\nu}}$ respectively and $\boldsymbol{\Xi = 1\!\!1}$.

Just as in the staggered fermion action, the gluon links used in the operators, are doubly stout links. We have kept the stout parameters of the action $(\omega_{A_1}, \omega_{A_2})$ distinct from the stout parameters of the operators $(\omega_{O_1}, \omega_{O_2})$, for wider applicability of the results.

RENORMALIZATION OF FERMION BILINEAR OPERATORS

The renormalization factors Z_Γ for lattice fermion bilinear operators, relate the bare operators $\mathcal{O}_{\Gamma_\circ} = \bar{\psi}\Gamma\psi$ to their corresponding renormalized continuum operators $\mathcal{O}_\Gamma$ via:

$$\mathcal{O}_\Gamma = Z_\Gamma\,\mathcal{O}_{\Gamma_\circ} \tag{16}$$

***RI′* scheme**: The renormalization condition in RI' scheme giving $Z_\Gamma^{L,RI'}$ (L: Lattice regularization) is:

$$\lim_{a\to0}\left[Z_\psi^{L,RI'}\,Z_\Gamma^{L,RI'}\,\Sigma_\Gamma^{(1)}(aq)\right]_{q^2=\bar{\mu}^2,\ m=0} = 1 \tag{17}$$

where $\bar{\mu}$ is the renormalization scale, Z_ψ is the renormalization factor for the fermion field ($\psi = Z_\psi^{-1/2}\,\psi_\circ$, $\psi(\psi_\circ)$: renormalized (bare) fermion field) and $\Sigma_\Gamma^{(1)}(aq)$ is a part of the **2-point amputated Green's functions of the operator $\boldsymbol{\mathcal{O}_{\Gamma_\circ}}$**, for each Γ:

$$\begin{aligned}
\boldsymbol{\Sigma_{\rm S}(aq)} &= 1\!\!1\ \boldsymbol{\Sigma_{\rm S}^{(1)}(aq)} && (18)\\
\boldsymbol{\Sigma_{\rm P}(aq)} &= \gamma_5\ \boldsymbol{\Sigma_{\rm P}^{(1)}(aq)} && (19)\\
\boldsymbol{\Sigma_{\rm V}(aq)} &= \gamma_\mu\ \boldsymbol{\Sigma_{\rm V}^{(1)}(aq)} + \frac{q^\mu \not{q}}{q^2}\ \boldsymbol{\Sigma_{\rm V}^{(2)}(aq)} && (20)\\
\boldsymbol{\Sigma_{\rm A}(aq)} &= \gamma_5\ \gamma_\mu\ \boldsymbol{\Sigma_{\rm A}^{(1)}(aq)} + \gamma_5\ \frac{q^\mu \not{q}}{q^2}\ \boldsymbol{\Sigma_{\rm A}^{(2)}(aq)} && (21)\\
\boldsymbol{\Sigma_{\rm T}(aq)} &= \gamma_5\ \sigma_{\mu\nu}\ \boldsymbol{\Sigma_{\rm T}^{(1)}(aq)} + \gamma_5\ \frac{\not{q}}{q^2}(\gamma_\mu q_\nu - \gamma_\nu q_\mu)\ \boldsymbol{\Sigma_{\rm T}^{(2)}(aq)} && (22)
\end{aligned}$$

where $\boldsymbol{\Sigma_\Gamma^{(1)} = 1 + \mathcal{O}(g_\circ^2)}$, $\boldsymbol{\Sigma_\Gamma^{(2)} = \mathcal{O}(g_\circ^2)}$, $g_\circ$: bare coupling constant. This scheme does not involve $\Sigma_\Gamma^{(2)}$; nevertheless, renormalizability of the theory implies that $Z_\Gamma^{L,RI'}$ will render the entire Green's function finite.

***RI′*-alternative scheme**: The renormalization condition in RI'-alternative scheme giving $Z_\Gamma^{L,RI'({\rm alter})}$ is:

$$\lim_{a\to0}\left[Z_\psi^{L,RI'}\,Z_\Gamma^{L,RI'({\rm alter})}\,\frac{{\rm tr}\big(\Gamma\Sigma_\Gamma(aq)\big)}{{\rm tr}\big(\Gamma\Gamma\big)}\right]_{q^2=\bar{\mu}^2,\ m=0} = 1 \tag{23}$$

where a summation over repeated indices μ and ν is understood. This scheme has the advantage of taking into account the whole bare Green's function and therefore is more appropriate for nonperturbative renormalization via numerical simulations where the arithmetic data for Σ_Γ cannot be separated into two different structures. RI' and RI'-alternative prescriptions differ between themselves (for V, A, T) by a finite amount.

$\overline{MS}$ scheme: The renormalization factors $Z_\Gamma^{L,\overline{MS}}$ for the operators $\mathcal{O}_{\Gamma_\circ}$ in $\overline{MS}$ scheme can be evaluated using the regularization independent conversion factors between RI' and $\overline{MS}$ schemes, as below:

$$\begin{aligned}
Z_\Gamma^{L,\overline{MS}} &= Z_\Gamma^{L,RI'}/C_\Gamma(g,\alpha),\ \text{for } \Gamma = \text{S, V, T} && (24)\\
Z_{\rm P}^{L,\overline{MS}} &= Z_{\rm P}^{L,RI'}/C_{\rm S}Z_5^{\rm P}, && (25)\\
Z_{\rm A}^{L,\overline{MS}} &= Z_{\rm A}^{L,RI'}/C_{\rm V}Z_5^{\rm A} && (26)
\end{aligned}$$

where $Z_5^{\rm P}(g)$ and $Z_5^{\rm A}(g)$ are additional finite factors, so that Pseudoscalar and Axial Vector operators satisfy the Ward identities; we also note that the value of Z_5^A for the flavor singlet operator differs from that of the nonsinglet one. The values of the conversion and "Z_5" factors are calculated in Refs. [11, 12].

FEYNMAN DIAGRAMS

There are 10 two-loop Feynman diagrams that enter in the computation of the 2-point amputated Green's functions of the operators, shown in Fig. 2. They all contain an operator insertion inside a closed fermion loop, and therefore vanish in the flavor nonsinglet case. Given that the difference between flavor singlet and nonsinglet operator renormalization first arises at two loops, we only need the tree-level values of Z_ψ, Z_g and of the conversion factors C_Γ, Z_5^P ($Z_\psi = Z_g = C_\Gamma = Z_5^P = 1$).

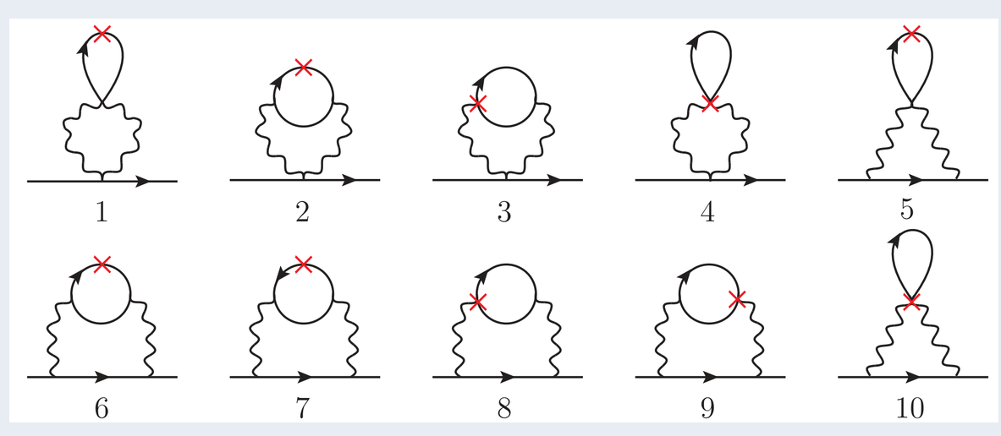

Figure 2: Diagrams contributing to the difference between flavor singlet and nonsinglet values of Z_Γ. Solid (wavy) lines represent fermions (gluons). A cross denotes insertion of the operator $\mathcal{O}_\Gamma$.

TREATMENT OF NONTRIVIAL DIVERGENT INTEGRALS

The different pole structure of the staggered fermion propagator gives rise to some nontrivial divergent integrals in the computation of the above two-loop diagrams. Particularly, there appeared 4 types of nontrivial divergent 2-loop integrals:

$$\begin{aligned}
I_{1\mu\nu} &= \int_{-\pi}^{\pi}\frac{d^4k}{(2\pi)^4}\frac{\mathring{k}_\mu\,\mathring{k}_\nu}{(\hat{k}^2)^2\ (\widehat{k+aq})^2}\int_{-\pi}^{\pi}\frac{d^4p}{(2\pi)^4}\frac{1}{\mathring{p}^2\ (\mathring{p+k})^2},\quad I_{2\mu\nu} = \int_{-\pi}^{\pi}\frac{d^4k}{(2\pi)^4}\frac{\mathring{k}_\mu\ \sin(aq_\nu)}{(\hat{k}^2)^2\ (\widehat{k+aq})^2}\int_{-\pi}^{\pi}\frac{d^4p}{(2\pi)^4}\frac{1}{\mathring{p}^2\ (\mathring{p+k})^2}\\
I_{3\mu\nu\rho\sigma} &= \int_{-\pi}^{\pi}\frac{d^4k}{(2\pi)^4}\frac{\mathring{k}_\mu\,\mathring{k}_\nu}{(\hat{k}^2)^2\ (\widehat{k+aq})^2}\int_{-\pi}^{\pi}\frac{d^4p}{(2\pi)^4}\frac{\sin(2p_\rho)\ \sin(2p_\sigma)}{(\mathring{p}^2)^2\ (\mathring{p+k})^2},\\
I_{4\mu\nu\rho\sigma} &= \int_{-\pi}^{\pi}\frac{d^4k}{(2\pi)^4}\frac{\mathring{k}_\mu\ \sin(aq_\nu)}{(\hat{k}^2)^2\ (\widehat{k+aq})^2}\int_{-\pi}^{\pi}\frac{d^4p}{(2\pi)^4}\frac{\sin(2p_\rho)\ \sin(2p_\sigma)}{(\mathring{p}^2)^2\ (\mathring{p+k})^2}
\end{aligned} \tag{27}$$

where $\hat{p}^2 = \sum_\mu \hat{p}_\mu^2$, $\hat{p}_\mu = 2\sin(p_\mu/2)$, $\mathring{p}^2 = \sum_\mu \mathring{p}_\mu^2$, $\mathring{p}_\mu = \sin(p_\mu)$ and q is an external momentum.

Proposed method: At first, we perform the substitution $p_\mu \to p'_\mu + \pi\ C_\mu$, where $-\pi/2 < p'_\mu < \pi/2$ and $C_\mu \in \{0,1\}$. Now the integration region for the innermost integral breaks up into 16 regions with range $[-\pi/2,\pi/2]$; the contributions from these regions are identical. To restore the initial range $[-\pi,\pi]$, we apply the following change of variables: $p'_\mu \to p''_\mu = 2p'_\mu$. Next, we apply subtractions of the form: $A(2k) = A(k) + [A_{\rm as}(2k) - A_{\rm as}(k)] + [A(2k) - A(k) - A_{\rm as}(2k) + A_{\rm as}(k)]$ and $B_{\rho\sigma}(2k) = \tilde{B}_{\rho\sigma}(2k) + [B_{\rho\sigma}(2k) - \tilde{B}_{\rho\sigma}(2k)]$, where

$$A(k) = \int_{-\pi}^{\pi}\frac{d^4p}{(2\pi)^4}\frac{1}{\hat{p}^2\ (\widehat{p+k})^2},\quad A_{\rm as}(k) \equiv \frac{1}{(4\pi)^2}[-\ln(k^2)+2] + P_2 \tag{28}$$

$$B_{\rho\sigma}(k) = \int_{-\pi}^{\pi}\frac{d^4p}{(2\pi)^4}\frac{\mathring{p}_\rho\ \mathring{p}_\sigma}{(\hat{p}^2)^2\ (\widehat{p+k})^2},\quad \tilde{B}_{\rho\sigma}(2k) \equiv \frac{1}{2(4\pi)^2}\frac{\mathring{k}_\rho\ \mathring{k}_\sigma}{\hat{k}^2} + \delta_{\rho\sigma}[\frac{1}{4}A(2k) - \frac{1}{32}P_1] \tag{29}$$

Then, we end up with standard (in the literature) divergent integrals [13–16] and convergent terms that we can integrate numerically for $a\to0$. The final expressions for the four integrals are given by:

$$\begin{aligned}
I_{1\mu\nu} =& \Big\{\frac{2}{(2\pi)^4}\Big[-\ln(a^2q^2)+\frac{3}{2}-\ln4\Big]+\frac{1}{2\pi^2}P_2\Big\}\frac{q_\mu q_\nu}{q^2} + \delta_{\mu\nu}\Big\{\frac{2}{(4\pi)^4}\Big[\ln(a^2q^2)\Big]^2\\
&-\frac{1}{4\pi^2}\Big[P_2+\frac{1}{(4\pi)^2}\Big(\frac{5}{2}-\ln4\Big)\Big]\ln(a^2q^2)-\frac{1}{4\pi^2}\Big[P_2+\frac{3}{2(4\pi)^2}\ln4\Big]+4X_2+G_1\Big\}+\mathcal{O}(a^2q^2)\\
I_{2\mu\nu} =& \Big\{\frac{1}{(2\pi)^4}\Big[\ln(a^2q^2)-2+\ln4\Big]-\frac{1}{\pi^2}P_2\Big\}\frac{q_\mu q_\nu}{q^2}+\mathcal{O}(a^2q^2)\\
I_{3\mu\nu\rho\sigma} =& \frac{1}{3(2\pi)^4}\frac{q_\mu q_\nu q_\rho q_\sigma}{q^4}+\delta_{\rho\sigma}\Big\{\frac{2}{(2\pi)^4}\Big[-\ln(a^2q^2)+\frac{5}{3}-\ln4\Big]-\frac{1}{(4\pi)^2}(P_1-8P_2)\Big\}\frac{q_\mu q_\nu}{q^2}\\
&+\frac{1}{12(2\pi)^4}\Big\{\delta_{\mu\nu}\frac{q_\rho q_\sigma}{q^2}+\delta_{\mu\rho}\frac{q_\nu q_\sigma}{q^2}+\delta_{\mu\sigma}\frac{q_\nu q_\rho}{q^2}+\delta_{\nu\rho}\frac{q_\mu q_\sigma}{q^2}+\delta_{\nu\sigma}\frac{q_\mu q_\rho}{q^2}\Big\}+\delta_{\mu\nu}\delta_{\rho\sigma}\Big\{\frac{2}{(4\pi)^4}\Big[\ln(a^2q^2)\Big]^2\\
&-\frac{1}{4\pi^2}\Big[P_2-\frac{1}{8}P_1+\frac{1}{(4\pi)^2}\Big(\frac{51}{2}-\ln4\Big)\Big]\ln(a^2q^2)-\frac{1}{4\pi^2}\Big[\Big(\frac{1}{3}-\ln4\Big)P_2-\frac{11}{144}P_1\\
&+\frac{3}{2(4\pi)^2}\Big(\frac{1}{27}-\ln4\Big)\Big]-\frac{1}{2}P_1\ P_2+4X_2+G_1+G_3\Big\}+(\delta_{\mu\rho}\delta_{\nu\sigma}+\delta_{\mu\sigma}\delta_{\nu\rho})\Big\{\frac{1}{(12\pi)^4}\Big[-\ln(a^2q^2)+\frac{1}{6}\Big]\\
&+\frac{1}{6\pi^2}(P_1+3P_2)+G_2\Big\}+\delta_{\mu\nu\rho\sigma}\Big\{\frac{1}{(2\pi)^4}+\frac{1}{2(4\pi)^2}-\frac{1}{3\pi^2}P_1+G_4\Big\}+\mathcal{O}(a^2q^2)\\
I_{4\mu\nu\rho\sigma} =& -\frac{1}{2(2\pi)^4}\frac{q_\mu q_\nu q_\rho q_\sigma}{q^4}-\frac{4}{(4\pi)^4}\Big\{\delta_{\mu\rho}\frac{q_\nu q_\sigma}{q^2}+\delta_{\mu\sigma}\frac{q_\nu q_\rho}{q^2}\Big\}+\delta_{\rho\sigma}\Big\{\frac{1}{(2\pi)^4}\Big[\ln(a^2q^2)-\frac{9}{4}\Big]-\frac{1}{2(2\pi)^2}(P_1-8P_2)\Big\}\frac{q_\mu q_\nu}{q^2}\\
&+\mathcal{O}(a^2q^2)
\end{aligned} \tag{30}$$

where P_1, P_2, X_2 are given in Ref. [13] and $G_1 = 0.000803016(6)$, $G_2 = -0.0006855532(7)$, $G_3 = 0.00098640(7)$ and $G_4 = 0.00150252(2)$.

RESULTS ON THE TWO-LOOP DIFFERENCE BETWEEN FLAVOR SINGLET AND NONSINGLET OPERATOR RENORMALIZATION

The contribution of the diagrams in Fig. 2 to $Z_{\rm P}$, $Z_{\rm V}$, $Z_{\rm T}$ vanishes identically just as in continuum regularizations. Unlike the case of Wilson fermions [1], Z_S also vanishes for staggered fermions; thus, only $Z_{\rm A}$ is affected. For the Axial Vector operator, our result can be written in the following form:

$$\begin{aligned}
&\boldsymbol{Z_{\rm A}^{\rm RI'(singlet)}(a\bar{\mu}) - Z_{\rm A}^{\rm RI'(nonsinglet)}(a\bar{\mu})} =\\
&-\frac{g_\circ^4}{(4\pi)^4}\,c_F\,N_f\Big\{6\ln(a^2\bar{\mu}^2)+\alpha_1+\alpha_2\,(\omega_{A_1}+\omega_{A_2})+\alpha_3\,(\omega_{A_1}^2+\omega_{A_2}^2)+\alpha_4\,\omega_{A_1}\,\omega_{A_2}\\
&+\alpha_5\,(\omega_{A_1}^3+\omega_{A_2}^3)+\alpha_6\,\omega_{A_1}\,\omega_{A_2}\,(\omega_{A_1}+\omega_{A_2})+\alpha_7\,(\omega_{A_1}^4+\omega_{A_2}^4)+\alpha_8\,\omega_{A_1}^2\,\omega_{A_2}^2\\
&+\alpha_9\,\omega_{A_1}\,\omega_{A_2}\,(\omega_{A_1}^2+\omega_{A_2}^2)+\alpha_{10}\,\omega_{A_1}^2\,\omega_{A_2}^2\,(\omega_{A_1}+\omega_{A_2})+\alpha_{11}\,\omega_{A_1}\,\omega_{A_2}\,(\omega_{A_1}^3+\omega_{A_2}^3)\\
&+\alpha_{12}\,\omega_{A_1}^3\,\omega_{A_2}^3+\alpha_{13}\,\omega_{A_1}^2\,\omega_{A_2}^2\,(\omega_{A_1}^2+\omega_{A_2}^2)+\alpha_{14}\,\omega_{A_1}^3\,\omega_{A_2}^3\,(\omega_{A_1}+\omega_{A_2})\\
&+\alpha_{15}\,\omega_{A_1}^4\,\omega_{A_2}^4+\alpha_{16}\,(\omega_{O_1}+\omega_{O_2})+\alpha_{17}\,\omega_{O_1}\,\omega_{O_2}+\alpha_{18}\,(\omega_{A_1}+\omega_{A_2})\,(\omega_{O_1}+\omega_{O_2})\\
&+\alpha_{19}\,\omega_{A_1}\,\omega_{A_2}\,(\omega_{O_1}+\omega_{O_2})+\alpha_{20}\Big[(\omega_{A_1}^2+\omega_{A_2}^2)\,(\omega_{O_1}+\omega_{O_2})+(\omega_{A_1}+\omega_{A_2})\,\omega_{O_1}\,\omega_{O_2}\Big]\\
&+\alpha_{21}\,(\omega_{A_1}^2+\omega_{A_2}^2)\,\omega_{O_1}\,\omega_{O_2}+\alpha_{22}\,(\omega_{A_1}^3+\omega_{A_2}^3)\,(\omega_{O_1}+\omega_{O_2})\\
&+\alpha_{23}\,\omega_{A_1}\,\omega_{A_2}\Big[(\omega_{A_1}+\omega_{A_2})\,(\omega_{O_1}+\omega_{O_2})+\omega_{O_1}\,\omega_{O_2}\Big]+\alpha_{24}\,(\omega_{A_1}^3+\omega_{A_2}^3)\,\omega_{O_1}\,\omega_{O_2}\\
&+\alpha_{25}\,\omega_{A_1}\,\omega_{A_2}\,(\omega_{A_1}^2+\omega_{A_2}^2)\,(\omega_{O_1}+\omega_{O_2})\\
&+\alpha_{26}\,\omega_{A_1}\,\omega_{A_2}\Big[\omega_{A_1}\,\omega_{A_2}\,(\omega_{O_1}+\omega_{O_2})+(\omega_{A_1}+\omega_{A_2})\omega_{O_1}\,\omega_{O_2}\Big]+\alpha_{27}\,\omega_{A_1}^2\,\omega_{A_2}^2\,\omega_{O_1}\,\omega_{O_2}\\
&+\alpha_{28}\,\omega_{A_1}\,\omega_{A_2}\Big[\omega_{A_1}\,\omega_{A_2}\,(\omega_{A_1}+\omega_{A_2})\,(\omega_{O_1}+\omega_{O_2})+(\omega_{A_1}^2+\omega_{A_2}^2)\,\omega_{O_1}\,\omega_{O_2}\Big]\\
&+\alpha_{29}\,\omega_{A_1}^3\,\omega_{A_2}^3\,(\omega_{O_1}+\omega_{O_2})+\alpha_{30}\,\omega_{A_1}^2\,\omega_{A_2}^2\,(\omega_{A_1}+\omega_{A_2})\,\omega_{O_1}\,\omega_{O_2}\\
&+\alpha_{31}\,\omega_{A_1}^3\,\omega_{A_2}^3\,\omega_{O_1}\,\omega_{O_2}\Big\}+\mathcal{O}(g_\circ^6)
\end{aligned} \tag{31}$$

where $c_F \equiv (N_c^2-1)/(2N_c)$ and N_f is the number of flavors. The numerical constants $\boldsymbol{\alpha_i}$ have been computed for various sets of values of the Symanzik coefficients; their values are listed in Table 2 for the **Wilson, tree-level (TL) Symanzik and Iwasaki gluon actions**.

	Wilson	TL Symanzik	Iwasaki		Wilson	TL Symanzik	Iwasaki
α_1	17.420(1)	16.000(1)	14.610(1)	α_{16}	24.9873(2)	18.0489(4)	9.9571(2)
α_2	-116.049(7)	-81.342(5)	-41.583(2)	α_{17}	-97.4550(2)	-62.2675(1)	-26.5359(1)
α_3	839.788(9)	539.121(6)	230.050(1)	α_{18}	-292.3650(5)	-186.8025(4)	-79.6078(2)
α_4	2175.14(3)	1394.12(2)	591.88(1)	α_{19}	4864.513(9)	2921.876(6)	1107.333(2)
α_5	-3462.830(1)	-2098.136(5)	-801.633(3)	α_{20}	1621.504(3)	973.959(2)	369.111(1)
α_6	-19565.9(1)	-11858.6(1)	-4528.6(1)	α_{21}	-10617.81(2)	-6122.11(1)	-2169.30(1)
α_7	6424.33(2)	3740.18(1)	1337.93(1)	α_{22}	-3539.269(6)	-2040.705(4)	-723.099(1)
α_8	200966.5(4)	117179.7(4)	41977.1(1)	α_{23}	-31853.42(5)	-18366.34(3)	-6507.89(1)
α_9	92171.5(3)	53720.8(1)	19237.6(1)	α_{24}	25847.14(3)	14435.59(2)	4881.52(1)
α_{10}	-1026448(1)	-580271(2)	-198722(1)	α_{25}	77541.41(1)	43306.78(6)	14644.54(2)
α_{11}	-183998.3(3)	-103929.7(3)	-35561.1(1)	α_{26}	232624.2(3)	129920.3(2)	43933.6(1)
α_{12}	5517230(30)	3037110(10)	1003641(1)	α_{27}	-1844375(1)	-1002465(1)	-326727(1)
α_{13}	2145810(10)	1180684(4)	389979(1)	α_{28}	-614791.6(6)	-334155.0(4)	-108909.0(2)
α_{14}	-11889300(40)	-6386950(30)	-2046240(10)	α_{29}	1736048.1(8)	920956.7(7)	290916.1(3)
α_{15}	26137700(200)	13729010(10)	4278680(10)	α_{30}	5208144(2)	2762870(2)	872748(1)
				α_{31}	-15545543(1)	-8065557(2)	-2478207(1)

Table 2: Numerical coefficients for the Axial Vector operator.

In the RI'-alternative scheme, the above result is modified by adding the finite term $\boldsymbol{\frac{g_\circ^4}{(4\pi)^4}\,c_F\,N_f}$. Also, in the $\overline{MS}$ scheme we must add the finite term $\boldsymbol{\frac{g_\circ^4}{(4\pi)^4}(-\frac{3}{2}c_F N_f)}$.

GRAPHS

The numerical value of the difference between singlet and nonsinglet renormalization functions can be very significant, depending on the values of the parameters employed in the action. In order to assess the importance of this difference, we present here several graphs of the results for certain values of c_i, ω_{A_1}, ω_{A_2}, ω_{O_1} and ω_{O_2}. The vertical axis of theses plots corresponds to $Z_A^{\rm diff.} \equiv \left[Z_A^{\rm (singlet)}(a\bar{\mu}) - Z_A^{\rm (nonsinglet)}(a\bar{\mu})\right]\left(-\frac{g_\circ^4}{(4\pi)^4}N_f c_F\right)^{-1}$ for $\bar{\mu} = 1/a$.

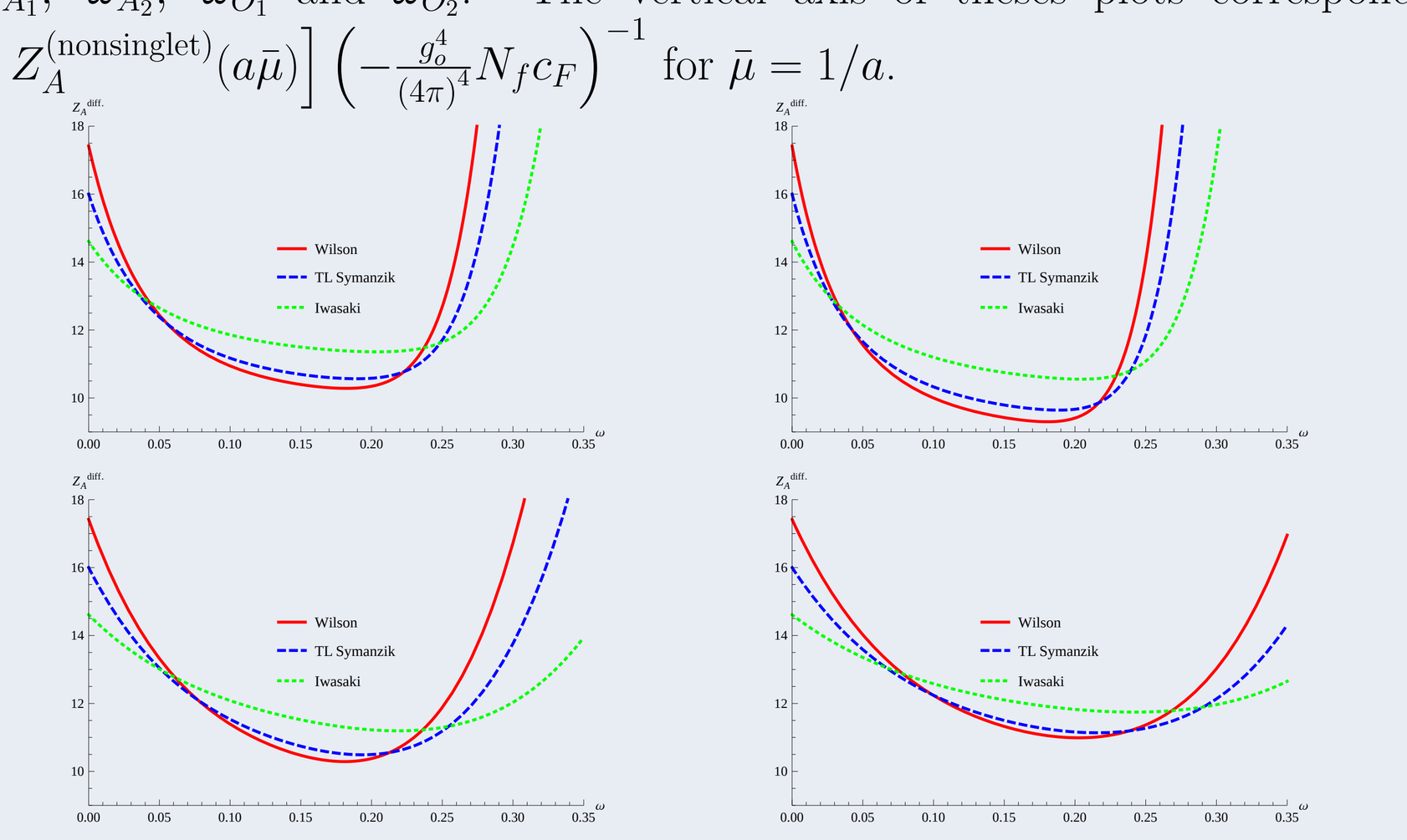

Figure 3: Plots of $Z_A^{\rm diff.}$, as a function of ω for the parameter values: upper left: $\omega_{A_1} = \omega_{A_2} = \omega_{O_1} = \omega_{O_2} = \omega$, upper right: $\omega_{A_1} = \omega_{A_2} = \omega$, $\omega_{O_1} = \omega_{O_2} = 0$, lower left: $\omega_{A_1} = \omega$, $\omega_{A_2} = \omega_{O_1} = \omega_{O_2} = 0$, lower right: $\omega_{A_1} = \omega_{O_1} = \omega$, $\omega_{A_2} = \omega_{O_2} = 0$.

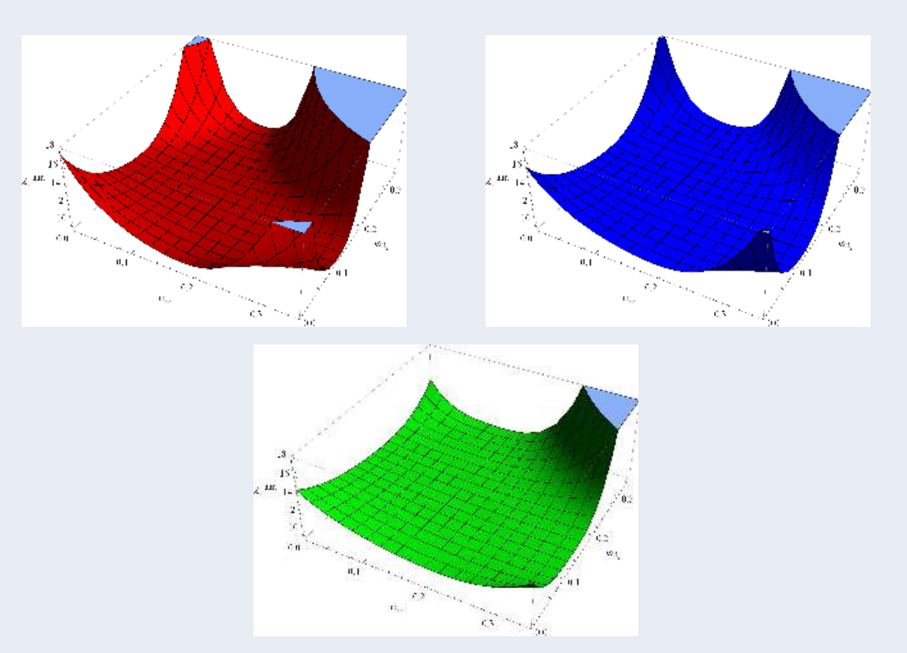

Figure 4: Plots of $Z_A^{\rm diff.}$, as a function of ω_{A_1} and ω_{A_2} for $\omega_{O_1} = \omega_{O_2} = 0$ (upper left: Wilson action, upper right: TL Symanzik action, lower: Iwasaki action).

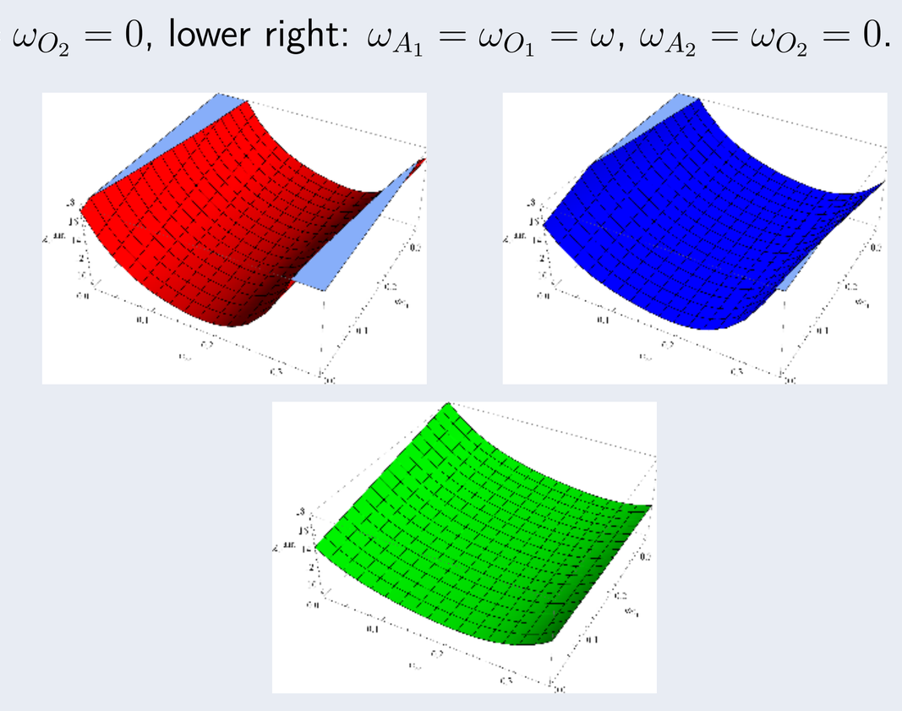

Figure 5: Plots of $Z_A^{\rm diff.}$, as a function of ω_{A_1} and ω_{O_1} for $\omega_{A_2} = \omega_{O_2} = 0$ (upper left: Wilson action, upper right: TL Symanzik action, lower: Iwasaki action).

We notice that the plots for the Iwasaki action are flatter than the remaining actions. Also, in Fig. 4 we notice that there is only one minimum, on the 45° axis. Therefore, the two smearing steps of the fermion action give better results than only one smearing step. Furthermore, we observe that the stout smearing of the action is more effective in minimizing $Z_A^{\rm diff.}$ than the stout smearing of operators.

REFERENCES

[1] M. Constantinou, M. Hadjiantonis, and H. Panagopoulos, PoS **LATTICE2014**, 298 (2014), [arXiv:1411.6990].

[2] M. Constantinou, M. Hadjiantonis, H. Panagopoulos, and G. Spanoudes, Phys. Rev. **D94**, 114513 (2016), [arXiv:1610.06744].

[3] A. J. Chambers et al. (QCDSF Collaboration) (2014), [arXiv:1410.3078].

[4] Y. Aoki, Z. Fodor, S. D. Katz, and K. Szabo, JHEP **0601**, 089 (2006), [hep-lat/0510084].

[5] Borsányi et al. (Wuppertal-Budapest Collaboration), J. Phys. **G38**, 124060 (2011), [arXiv:1109.5030].

[6] A. Bazavov et al. (MILC Collaboration) (2012), [arXiv:1212.4768].

[7] M. Constantinou, M. Costa, and H. Panagopoulos, Phys. Rev. **D88**, 034504 (2013), [arXiv:1305.1870].

[8] C. Morningstar and M. J. Peardon, Phys. Rev. **D69**, 054501 (2004), [hep-lat/0311018].

[9] R. Horsley, H. Perlt, P. E. L. Rakow, G. Schierholz, and A. Schiller (QCDSF Collaboration), Nucl. Phys. **B693**, 3 (2004), [Erratum: Nucl. Phys. B713, 601(2005)], [hep-lat/0404007].

[10] A. Patel and S. R. Sharpe, Nucl. Phys. **B395**, 701 (1993), [hep-lat/9210039].

[11] J. A. Gracey, Nucl. Phys. **B662**, 247 (2003), [hep-ph/0304113].

[12] S. A. Larin, Phys. Lett. **B303**, 113 (1993), [hep-ph/9302240].

[13] M. Lüscher and P. Weisz, Nucl. Phys. **B452**, 234 (1995), [hep-lat/9505011].

[14] K. Chetyrkin and F. Tkachov, Nucl. Phys. **B192**, 159 (1981).

[15] H. Panagopoulos and E. Vicari, Nucl. Phys. **B332**, 261 (1990).

[16] R. Ellis and G. Martinelli, Nucl. Phys. **B235**, 93 (1984).